

THE EFFECT OF POLYMERS ON THE DYNAMICS OF TURBULENCE IN A DRAG REDUCED FLOW

by

**Jovan JOVANOVIĆ, Bettina FROHNAPFEL,
Mira PASHTRAPANSKA, and Franz DURST**

Original scientific paper
UDC: 532.57:519.876.5:541.64
BIBLID: 0354-9836, 9 (2005), 1, 13-41

An experimental investigation of a polymer drag reduced flow using state-of-the-art laser-Doppler anemometry in a refractive index-matched pipe flow facility is reported. The measured turbulent stresses deep in the viscous sublayer are analyzed using the tools of invariant theory. It is shown that with higher polymer concentration the anisotropy of the Reynolds stresses increases. This trend is consistent with the trends extracted from DNS data of non-Newtonian fluids yielding different amounts of drag reduction. The interaction between polymer and turbulence is studied by considering local stretching of the molecular structure of a polymer by small-scale turbulent motions in the region very close to the wall. The stretching process is assumed to re-structure turbulence at small scales by forcing these to satisfy local axisymmetry with invariance under rotation about the axis aligned with the main flow. It is shown analytically that kinematic constraints imposed by local axisymmetry force turbulence near the wall to tend towards the one-component state and when turbulence reaches this limiting state it must be entirely suppressed across the viscous sublayer. Based on this consideration it is suggested that turbulent drag reduction by high polymers resembles the reverse transition process from turbulent to laminar. Theoretical considerations based on the elastic behavior of a polymer and spatial intermittency of turbulence at small scales enabled quantitative estimates to be made for the relaxation time of a polymer and its concentration that ensure maximum drag reduction in turbulent pipe flows, and it is shown that predictions based on these are in very good agreement with available experimental data.

Key words: *turbulent drag reduction, polymers, transition, turbulence, boundary layer, internal flows*

Introduction

The addition of small amounts of dilute polymers to wall bounded flows can lead to large drag reduction (DR). This phenomena has received much attention since its discovery more than 50 years ago. Nevertheless, detailed knowledge about the chief mechanism for the action of the polymer and its effect on turbulence is not available.

In respect to important research efforts in this field the early studies of Metzner and Park [1], Lumley [2, 3], Virk [4], Berman [5], and the more recent contributions of Tabor and Gennes [6], Ryskin [7], Thirumalai and Bhattacharjee [8], and Sreenivasan and White [9] should be mentioned. Turbulence measurements in drag reduced flow only became possible with the development of advanced optical measuring techniques. The experimental work of Rudd [10] and Logan [11], and subsequent contributions of Reischman and Tiederman [12], Luchik and Tiederman [13], Walker and Tiederman [14], Willmarth *et al.* [15], Wei and Willmarth [16], and Warholic *et al.* [17] provided important information on modifications of the statistical properties of turbulence in wall-bounded flows by presence of polymer additives. Most of these experimental investigations were carried out for a low percentage of DR. The mean velocity profile was found not to follow a classical log law. The root mean square of the streamwise and normal velocity fluctuations, normalized with the wall friction velocity determined for the polymer flow, were larger and lower, respectively, than in Newtonian liquid. These trends became more pronounced as DR increased. For large DR, experiments showed that the turbulent shear stress is approximately zero, indicating that turbulence is not maintained by the well-known mechanism (which ensures that rates of energy generation and viscous dissipation are in balance) and that the persistence of turbulence is associated with the statistical dynamics of extra polymer stresses.

In order to gain a more detailed insight into the phenomena of polymer drag reduction, direct numerical simulations have been performed by Toonder *et al.* [18], Sureshkumar *et al.* [19], Dimitropoulos *et al.* [20], Sibilla and Baron [21], Angelis *et al.* [22], and Dubief *et al.* [23, 24]. These numerical studies provided considerable information about the behaviour of turbulence in presence of a polymer solution in the flow: the influence of a polymer on the mean flow and turbulence stresses and their detailed budgets including instantaneous three-dimensional flow patterns. These simulations, like those of Newtonian turbulence, cannot themselves lead to improved understanding without a firm theory capable of distinguishing the cause from the consequence. A lack of generally accepted and well-supported theory for the remarkable evidence that one drop of a long-chain polymer properly mixed with a few hundred liters of liquid can reduce up to 80% of friction drag in a pipe flow illustrates the huge gap that exists in our current knowledge of wall turbulence. This situation immediately suggests that something substantial and very fundamental can be learned about turbulence by studying the mechanism of polymer drag reduction.

The theory of turbulent drag reduction in simple, nearly parallel wall-bounded flows can be worked out proceeding from the basic equations that govern the turbulent stresses and by using (*but not misusing*) the turbulence closure based on the application of the two-point correlation technique and invariant theory [25]. Conclusions emerging from the theory can be tested by direct comparisons with numerical simulations or experiments. The mechanism responsible for large drag reduction can be identified without appeal to the empirical input or auxiliary approximation. However, its description might not be digestible for those who reason about turbulence (in a deterministic fashion) exclusively in the physical space where observations usually take place: exposition and usage of arguments and resulting deductions may therefore seem unreasonable, confusing or

entirely wrong. If the matter is analysed in the functional space formed by the two scalar invariants which emphasize the anisotropy of turbulence, the problem of large drag reduction turns out to be the first one to attack because of its simplicity and specific and unconventional usage of arguments then appear logical and transparent. By arguing in the real space and the functional space it was possible to specify this interaction in the form of kinematic constraints and to show how these constraints force suppression of turbulence close to the wall, leading to significant drag reduction.

In this paper we present experimental investigations of turbulent drag reduction using polymer additives. The base of this investigation came out of the work of Jovanović and Hillerbrand [26] in connection with the flow control of a laminar boundary layer at very high Reynolds numbers. The performed experiments confirmed the major conclusion which emerged from the above-mentioned theoretical work, namely that the mechanism of drag reduction is associated with an increase in anisotropy of turbulence at the wall.

This paper also provides consideration of the two most important issues related to maximum turbulent drag reduction for pipe flows: determination of the relaxation time of a polymer and its concentration. Following the elastic theory, the relaxation time of a polymer (t_{pol}) is determined by requiring that it should be larger than the characteristic time-scale of turbulent motions in the dissipation range (t_K). Since the small-scale structure of turbulence in the dissipation range is universal, the concentration of a polymer is determined from its spatial extent using well-established relations which hold in isotropic turbulence and the experimental evidence that the mean separation between regions associated with motions at Kolmogorov's scale is comparable to the integral length-scale of turbulence.

Experimental investigation of polymer drag reduction

The conclusion emerging from the theoretical work of Jovanović and Hillerbrand [26] is that the effective way to suppress small-scale fluctuations in the near-wall region is to force them to be predominantly one-component. To verify whether this implication also holds for polymer drag reduction, an experimental programme using state-of-the-art laser-Doppler (LDA) measuring technique was initiated. This technique allows accurate experimental data to be obtained deep inside the viscous sublayer, enabling a quantitative basis to be formed for the interpretation of the dynamics of turbulence using the tools of invariant theory.

Test section and instrumentation

Measurements were performed in the refractive index-matched pipe-flow facility at the Lehrstuhl für Strömungsmechanik in Erlangen. This test rig has been used extensively for different LDA measurements. It is a closed-loop pipe flow installation driven by a screw conveyor pump. Flow rates between 0.6 and 20 m³h⁻¹ can be achieved with a tolerance of 1%.

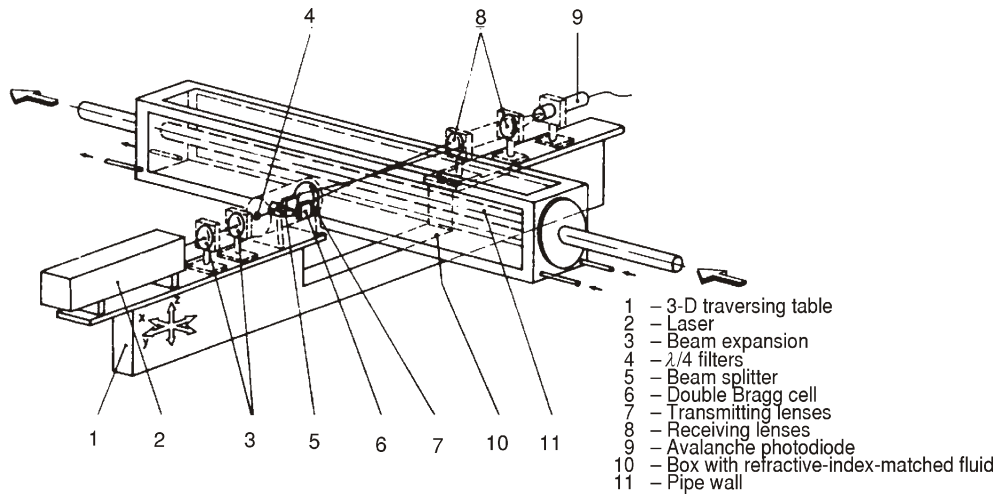


Figure 1. Layout of the LDA optical system

With a pipe diameter of 50 mm a maximum Reynolds number of $Re = 4.4 \cdot 10^4$ can be realized. The test section is located about 4 m downstream, providing a development length of about 100 pipe diameters. In the present experiments, the flow was tripped at the pipe inlet to ensure additionally fully developed flow conditions. A more detailed description of the experimental apparatus can be found in Durst *et al.* [27].

The arrangement of the LDA optical system and the test section is shown in fig. 1. The optical system consisted of a 15 mW helium-neon laser and a double Bragg cell unit. In the near-wall region measurements were performed with the Bragg cells operated at 40.0 and 40.3 MHz, providing a shift frequency of 300 kHz. The measuring control volume was about 60 μm in diameter (minor axis d_2) and had a length of 230 μm (major axis d_1). These values, based on the e^{-2} intensity cut-of point, were calculated from:

$$d_2 = \frac{4\lambda f}{E\pi d_{\text{beam}} \cos \varphi} \quad (1)$$

and

$$d_1 = \frac{4\lambda f}{E\pi d_{\text{beam}} \sin \varphi} \quad (2)$$

where E is the beam expansion factor, λ the laser wavelength, f the focal length of the transmitting lens, d_{beam} the diameter of the unfocused laser beam and φ half the intersection angle of the beams.

Although a fully developed state of turbulence at the measuring station had to be ensured, the facility was not operated at maximum speed, because the thickness of the viscous sublayer decreased with increasing mean flow velocity. To allow measurements in the direct proximity of the wall, a Reynolds number of $2.5 \cdot 10^4$ was chosen.

To quantify drag reduction, which is defined as:

$$DR = 1 - \frac{\tau_{w, pol}}{\tau_w} \quad (3)$$

it was necessary to determine the wall shear stress τ_w . This was accomplished by measuring the mean velocity at a fixed and predetermined position from the wall within the viscous sublayer.

In order to analyse the structure of turbulence in a DR flow using invariant theory, the second-order moments are required. For measurements in the viscous sublayer ($x_2 = 5$) it is possible to plot data in the anisotropy invariant map using axial and tangential fluctuation values only. Figure 2 shows direct numerical simulation (DNS) results of Mansour *et al.* [28] for $x_2 = 5$ plotted in the anisotropy invariant map: once using all Reynolds stress components and once using the u_1^2 and u_3^2 components only. It can be seen that there is no significant difference in the values obtained. Therefore, the mean velocity and the fluctuating components u_1^2 in axial and u_3^2 in tangential direction at a fixed position inside the region of the viscous sublayer were sufficient for the purpose of this investigation.

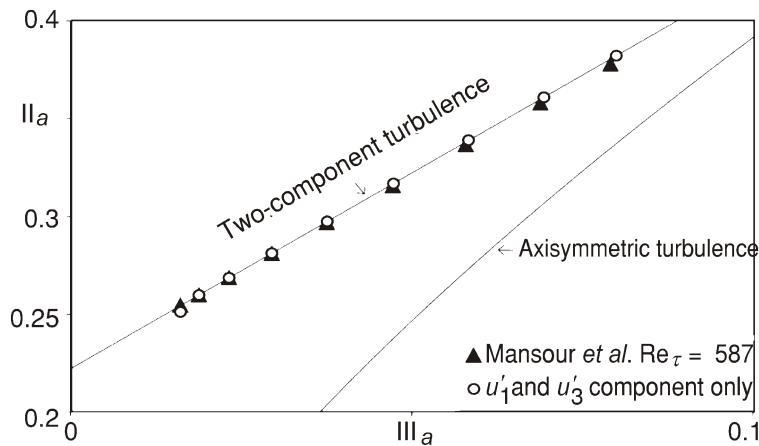


Figure 2. DNS data from Mansour *et al.* [28] for $x_2 = 5$ plotted on the expanded scale in the anisotropy invariant map

Turbulent pipe flow without polymer additives

Preliminary measurements without the addition of polymer additives were performed to verify the measured quantities. For velocity measurements in the axial direction, the LDA system was traversed in the vertical direction. By rotating the transmitting optics by 90° , the tangential velocity component u_3^2 was measured in the horizontal plane. In order to obtain statistically accurate results, measurements were taken for 4 minutes at each point. This period corresponds almost to the time during which the entire oil circulated once through the experimental loop and therefore cannot be selected higher.

The wall shear velocity u_τ was calculated from the slope of the measured mean velocity profile in the viscous sublayer. Additionally, u_τ was estimated from the Clauser diagram ($u = 0.08088 \text{ m s}^{-1}$) and using the Blasius formula for the friction coefficient:

$$\frac{\tau_w}{\frac{1}{2}\rho\bar{U}_B^2} = 0.0791 \frac{\bar{U}_B D}{\nu}^{1/4} \quad (4)$$

With a bulk velocity of $\bar{U}_B = 1.40 \text{ ms}^{-1}$ the wall shear velocity yields $u_\tau = 0.07968 \text{ ms}^{-1}$. This value deviates less than 2% from the calculated value of $u_\tau = 0.08096 \text{ ms}^{-1}$.

For axial turbulence intensity measurements, the expression [27]:

$$\frac{\overline{u_{1\text{meas}}^2}}{\overline{u_{1\text{true}}^2}} = \frac{d_2^2}{16} \frac{d^2 \overline{U}_1}{dx_2}^2 \quad (5)$$

was used for correcting the measured data for the finite size of the measuring control volume. The resulting corrections were of the order of less than 8% in the near-wall region. The mean velocity does not require a correction since the leading term of the correction represents the curvature of the velocity profile, which is negligible close to the wall. Figure 3 confirms the linear dependence of the mean velocity \overline{U}_1 and of the corrected turbulence intensity u_1^2 on the dimensionless wall distance $x_2 = x_2 u_\tau / \nu$. Since the mean velocity in the tangential direction is approximately zero, no corrections concerning the finite size of the measuring control volume had to be applied to u_3^2 .

In fig. 4, the local mean velocity is plotted with respect to the dimensionless wall distance. Comparison with the universal law of the wall, experimental data of Durst *et al.* [27] and DNS results shows good agreement. Figure 5 shows the local root mean square values of the axial fluctuation component normalized with the wall shear velocity as a function of the dimensionless wall distance. These measurements compare well with available DNS results and experiments reported by Durst *et al.* [27].

For measurements of the fluctuating component in the tangential direction $\overline{u_3^2}$, the optical system was arranged in such a way that the major axis of the elliptical measuring volume was normal to the wall. Therefore, the spatial resolution in the tangential

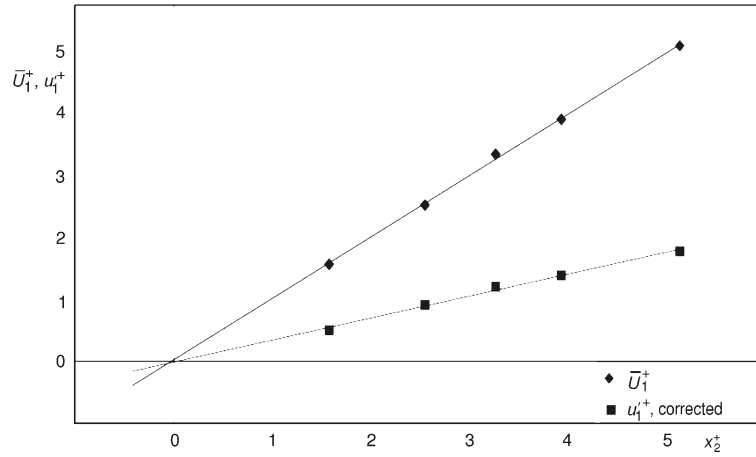


Figure 3. Velocity profile and turbulent intensity profile in the region very close to the wall

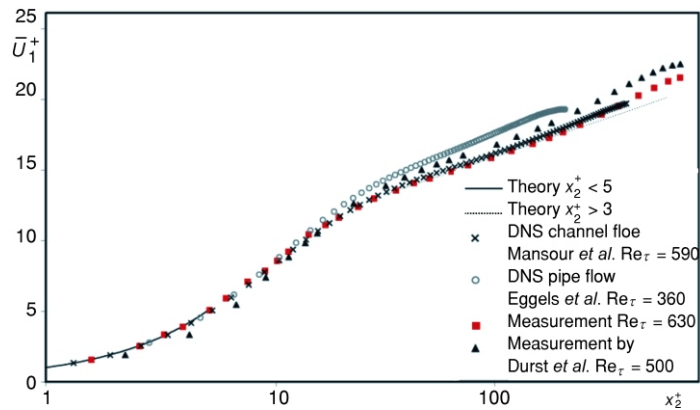


Figure 4. Local mean velocity versus dimensionless distance from the wall: comparison with the universal law of the wall, DNS results and experimental results of Durst *et al.* [27]

direction was limited and prevented measurements closer than $\sim 230 \mu\text{m}$ from the wall. Figure 6 shows comparisons of experimental results with those obtained from numerical simulations and the measurements reported by Durst *et al.* [27], which were performed at the same test rig. It can be seen that measurement errors exist in the region $x_2 = 10$. The dimensionless size of the measuring volume was:

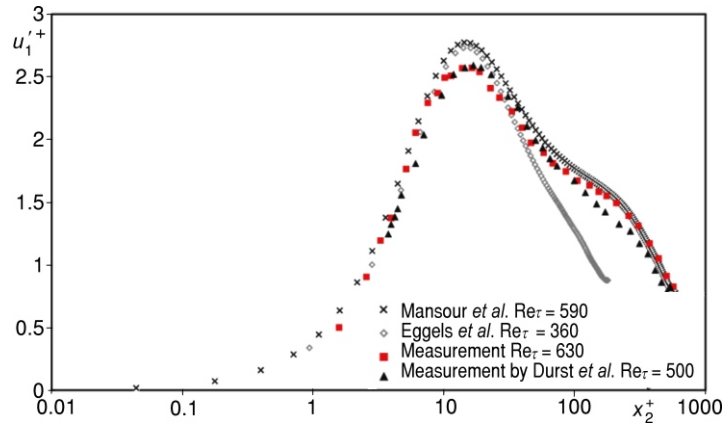


Figure 5. Axial turbulent intensity component u_1' : comparisons with DNS results and experimental results of Durst *et al.* [27]

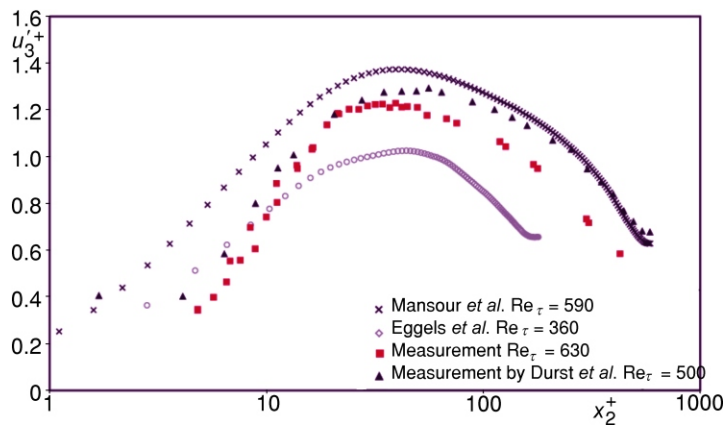


Figure 6. Tangential intensity component u_3' : comparisons with DNS results and experiment of Durst *et al.* [27]

$$d_1 \frac{d_1 u_\tau}{\nu} \approx 6 \quad (6)$$

which indicates that it covered not only the near-wall region but also parts of the wall. With the addition of polymers, u_τ decreases drastically. Therefore, the dimensionless size of the measuring volume decreases and correct measurements of the tangential intensity component in the near-wall region become possible.

Turbulent flow with polymer additives

The polymer can be added to the flow in different ways. It can be injected into the flow at different concentrations or a homogeneous mixture can be prepared in advance. In order to guarantee a homogeneous mixture from the start it was decided to prepare the mixture outside the installation. A 50 ppm solution of a FORTUM* polymer, illustrated in fig. 7, mixed with Diesel oil was prepared. This mixture was stirred slowly for 1 week before distributing it to four 200 l kegs of Diesel oil yielding 5 and 10 ppm solutions, respectively. These solutions were stirred for another 24 h before being returned to the installation. Since the polymer is sensitive to mechanical straining, all these steps were performed very carefully and slowly. The viscosity was measured for the pure mixture of the two Diesel oils and the 50 ppm solution, yielding a constant kinematic viscosity of $\nu = 3.2 \cdot 10^{-6} \text{ ms}^{-2}$.

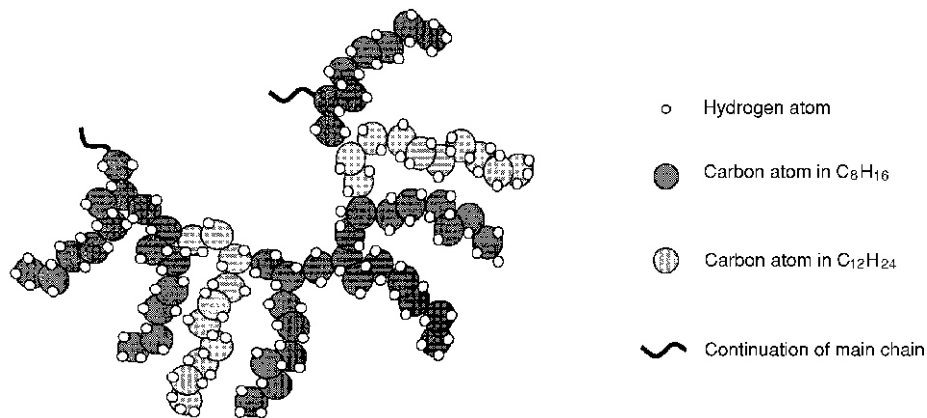


Figure 7. Illustration of the molecular structure of a FORTUM polymer sample after Koskinen [29]: $M = 25 \cdot 10^6 \text{ g mol}^{-1}$, $M_{\text{dodecane}} = 168.4320 \text{ g mol}^{-1}$, $M_{\text{octane}} = 112.2880 \text{ g mol}^{-1}$, $l = 2 \times 1.54 \text{ \AA}$, $r_{d/o} = C_{12}H_{24}/C_8H_{16} = 1/3$, $N_{\text{monomer}} = M_{\text{polymer}}/[r_{d/o}M_{\text{octane}} + (1 - r_{d/o})M_{\text{dodecane}}]$

Since the polymer solution showed a rather short lifetime, with detectable degradation effects after 1 h of continuous operation, it was not possible to obtain the entire velocity profile of the flow in one session of measurements. Owing to the elaborate preparation procedure of the polymer solutions, the measurement of the entire velocity profile was abandoned and measurements at one point inside of the viscous sublayer were taken until the polymer had degraded and no further drag reduction could be observed. At regular time intervals, a sample of a working fluid was taken in order to check its kinematic viscosity, which was found to maintain a constant value.

* FORTUM Power and Heat Oy, P. O. Box 20, 00048 FORTUM, Finland

Mean velocity and turbulence intensities in axial and tangential directions were measured for each of the solutions. Measurements were taken for about 10 h. Subsequently, the exact location of the measurement control volume was verified.

Results of the measurements with polymer additives are presented in figs. 8-10. The higher the concentration of the polymer, the lower is the velocity. This implies a less steep velocity gradient at the wall, as expected for a drag reduced flow. As time passes,

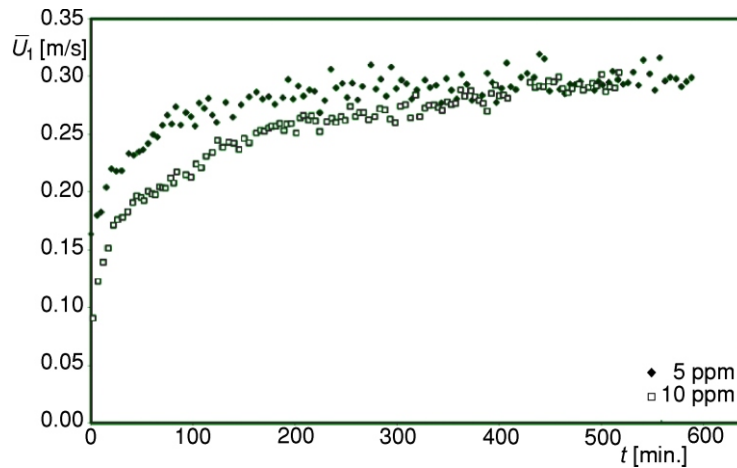


Figure 8. Behaviour of the mean velocity with time for degrading polymer solutions

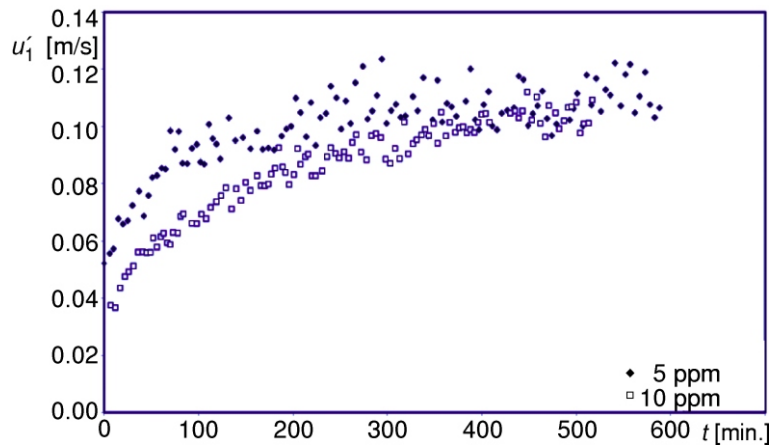


Figure 9. Behaviour of the axial turbulent intensity component in degrading polymer solutions

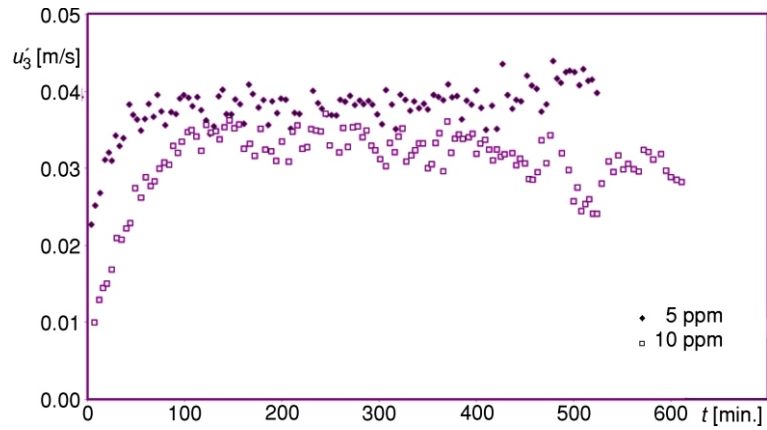


Figure 10. Behaviour of the tangential turbulent intensity component in degrading polymer solutions

the influence of the polymer vanishes and the value of the velocity increases until a steady value is reached. The same trend can be observed in histories of the turbulence intensities.

As shown in fig. 11, DR decreased fast within the first 2 h. With an addition of 10 ppm polymers a maximum DR of 70% could be observed. The effect had completely vanished after continuous operation for 7.5 h. The highest value of DR with a 5 ppm polymer concentration was around 50%. For this concentration of a polymer, the effect had disappeared 4 h after the beginning of the measurements.

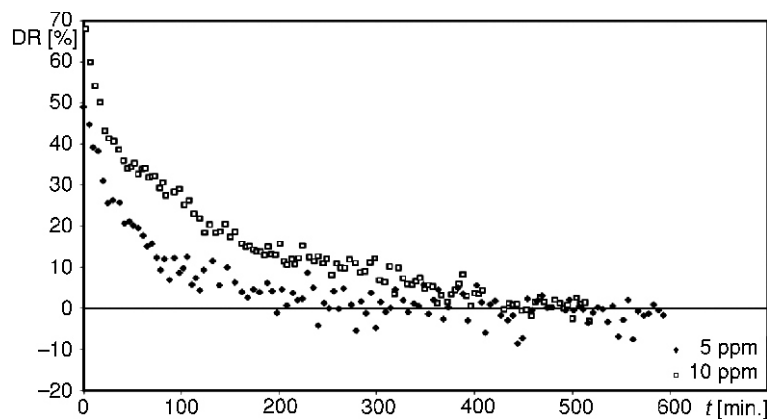


Figure 11. DR for different concentrations of a polymer

The measured data were analysed by plotting these on the anisotropy invariant map. Figure 12 shows the obtained results. The position of the initial point in the anisotropy invariant map depends on the polymer concentration and induced DR. With higher concentrations of a polymer its location moves closer to the one-component limit. As shown earlier, the same trend can be observed in Newtonian fluids for decreasing Reynolds numbers (see fig. 17). As time passes, the data indicate a clear tendency to move downwards along the two-component state from a position close to the one-component limit towards the isotropic two-component limit. These trends in the anisotropy invariant map lasted about 25 and 80 min. for polymer concentrations of 5 and 10 ppm respectively, before the trend in the data reversed direction on the anisotropy map. The reversed trend in the data corresponds roughly to a remaining DR of about 30%.

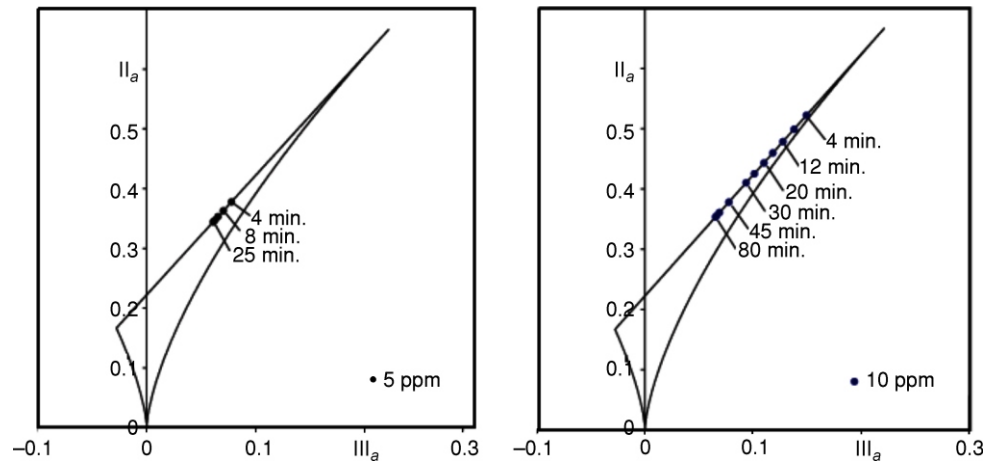


Figure 12. Measurement results plotted on the anisotropy invariant map (together with those shown in previous figure) demonstrate that with decreasing DR the data points move away from the one-component limit

This reversed trend has no physical explanation but is caused by a reduced resolution in measurements due to the degradation of the polymer. Owing to polymer addition, the wall shear velocity u_τ decreased drastically. Thus, the initial dimensionless size of the measuring control volume was calculated to be:

$$d_1 = \frac{d_1 u_{\tau, \text{initial}}}{\nu} \approx 3.2 \quad (7)$$

so that precise measurements in the viscous sublayer with $x_2 = 5$ were possible. With degradation of the polymer u_τ increased and also the dimensionless size of the measured

control volume. At the point of 30% DR, the major axis d_1 assumed a value larger than the thickness of the viscous sublayer. For this reason, measurements in the viscous sublayer did not yield correct results for a low percentage of DR.

Figure 13 shows that this trend is confirmed by data from direct numerical simulations of drag reduced, fully turbulent flows. The trajectories of the joint variation of the invariants of a_{ij} across the anisotropy-invariant map from the numerical database of a turbulent channel flow from Dimitropulos *et al.* [20] are presented and it can be seen that that with increasing DR, which is accompanied by suppression of wall turbulence [17], the point that corresponds to the position at the wall $x_2 = 0$ moves upwards in the direction of the one-component limit.

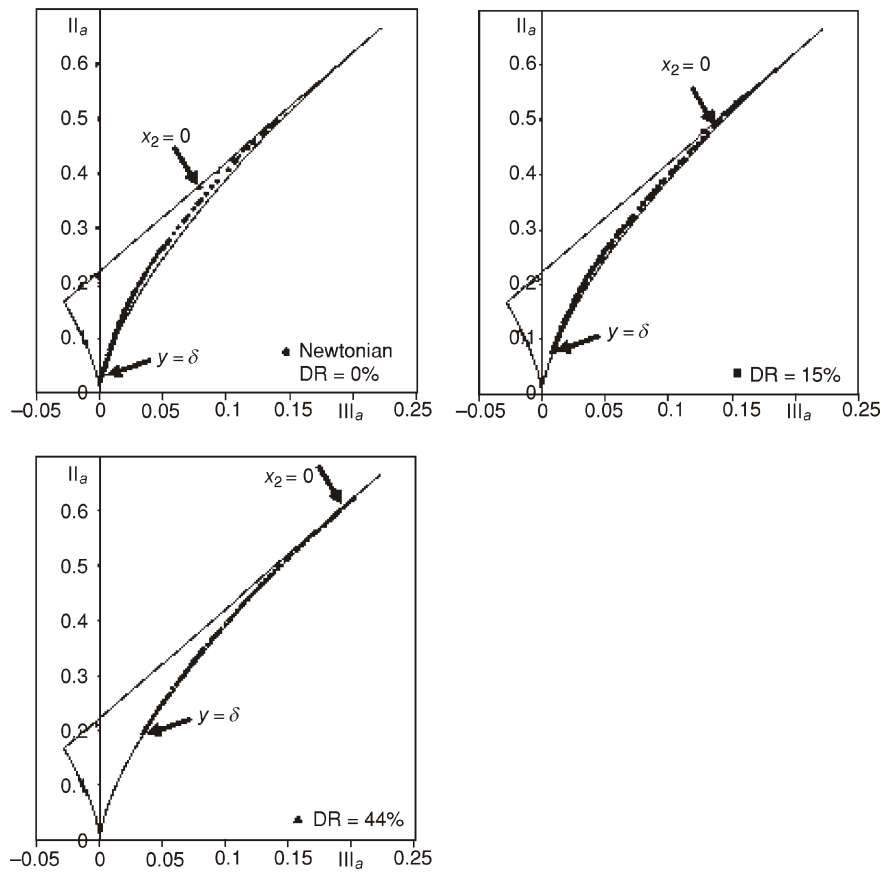


Figure 13. Anisotropy-invariant mapping of turbulence in a fully developed channel flow with DR from direct numerical simulations of Dimitropulos *et al.* [20]. The trend in the data at the wall ($x_2 = 0$) strongly supports the conclusion that DR increases as turbulence approaches the one-component limit

The mechanism of polymer drag reduction

The problem of polymer DR remains poorly understood mainly because the interaction between a polymer and turbulence is essentially at the molecular level of the former. This interaction involves modification of the molecular structure of a polymer by turbulent motions in the near-wall region. Figure 14 shows a conceptual scenario where, under very special circumstances, turbulence in the near-wall region forces rolled-up chains of a polymer partially to unroll and stretch in the mean flow direction.

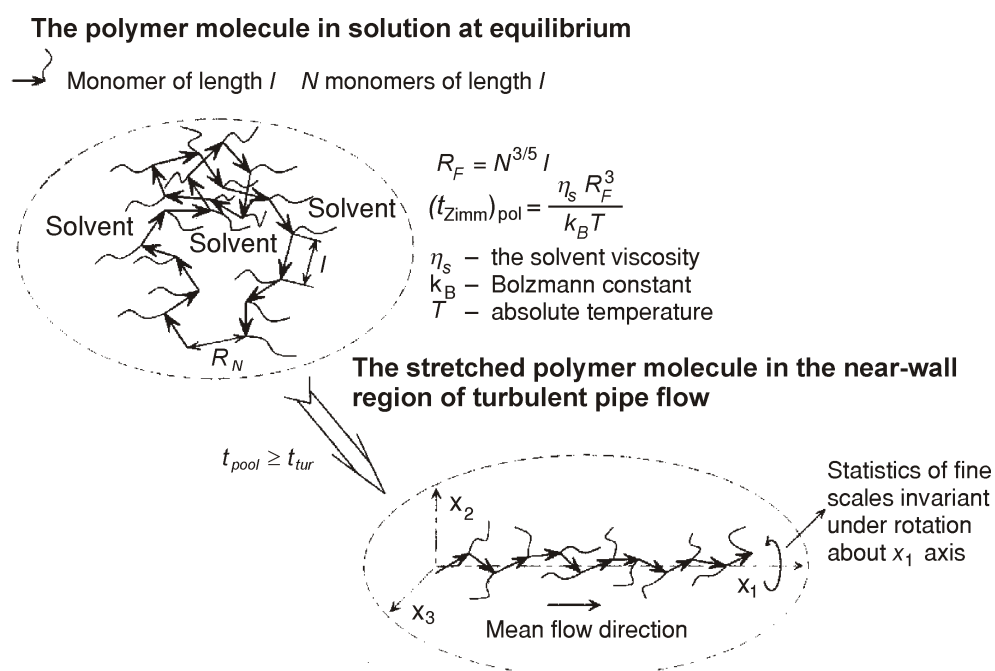


Figure 14. Behaviour of a polymer in solution at equilibrium (top) and its response to stretching by turbulent motions at small scales very close to the wall (bottom). Here R_N and R_F are hydrodynamical and Flory radius, respectively

In the unrolled state, polymer chains dictate characteristic length scales associated with the fine structure of turbulence. These scales are elongated in the streamwise direction and are therefore strongly anisotropic. In the most extreme case, polymer chains form a filament structure with a length-scale arrangement which is almost axisymmetric around the axis aligned with the mean flow. Hence it is reasonable to assume that the chief mechanism of DR is related to the ability of the activated polymer to re-structure turbulence at small scales by forcing them to satisfy constraints imposed by local axisymmetry. Local axisymmetry as illustrated in fig. 14 requires that the statistics of

higher order velocity derivatives, which contribute to the turbulent dissipation correlations, must satisfy invariance under rotation about the axis orientated in the mean flow direction.

In the near-wall region, the presence of the polymer increases not only the anisotropy in length scales but also anisotropies in the dissipation and turbulent stresses, since these are closely related across the viscous sublayer. This can be shown using the two-point correlation technique and invariant theory [25]. If the polymer concentration (c) and its relaxation time (t_{pol}) are appropriately matched to the properties of turbulence, it will undergo considerable modification and reach, at the wall, a state of maximum anisotropy. This state can be identified on the anisotropy-invariant map shown in fig. 15 and corresponds to the one-component limit ($\Pi_a = 2/3$). For these limiting conditions Jovanović and Hillerbrand [26] provided an analytical proof which shows that if turbulence (at

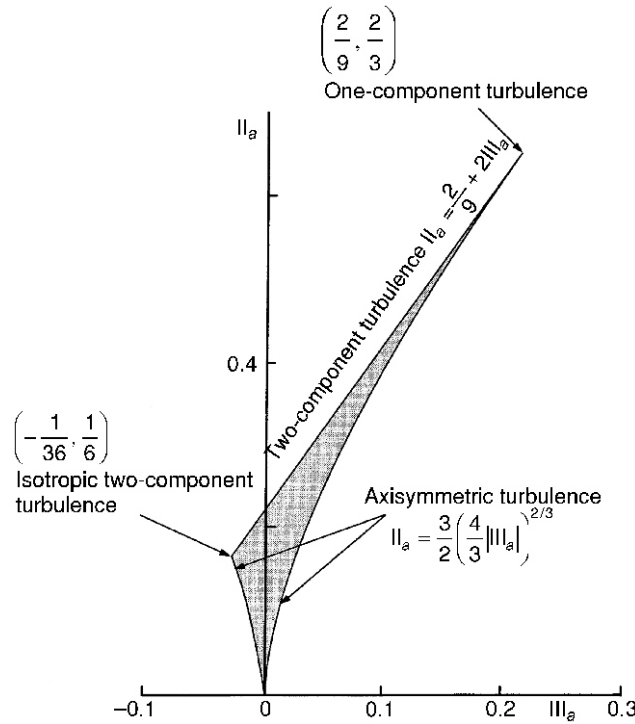


Figure 15. Anisotropy-invariant map of the tensor $a_{ij} = \overline{u_i u_j} / q^2 - 1/3 \delta_{ij}$ and the limiting values of scalar invariants $\Pi_a = a_{ij} a_{ji}$ and $\text{III}_a = a_{ij} a_{jk} a_{ki}$ for the different states of the turbulence, after Lumley and Newmann [30]. Here $\overline{u_i u_j}$ is the Reynolds stress tensor and q^2 is its trace $q^2 = \overline{u_s u_s}$. According to Lumley [31], all realistic turbulence must exist within the area delimited by the map

small scales) close to the wall is locally axisymmetric as illustrated in fig. 14, it must undergo very rapid laminarization and therefore considerable DR owing to suppression of the turbulent dissipation rate ε , which, under common circumstances, reaches a maximum at the wall (see fig. 16).

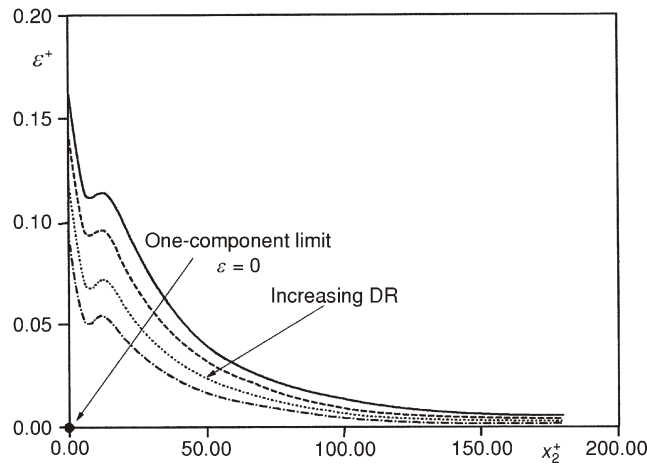


Figure 16. Distribution of the turbulent dissipation rate ε versus distance from the wall, normalized on the inner variables u_τ and ν , in a plane channel flow (DR = 0) from direct numerical simulations of Kim *et al.* [33], sketched ε profiles for non-vanishing DR and the limiting state at the wall for maximum DR

For an extreme situation, when $(\Pi_a)_{\text{wall}} = 2/3$ and $(\varepsilon)_{\text{wall}} = 0$, the statistical dynamics of the turbulent stresses constructed by combining the two-point correlation technique and invariant theory written in Cartesian notation [25]*:

$$\frac{\partial \overline{u_1^2}}{\partial t} = P_{11} - a_{11} P_{ss} - \mathcal{F} \frac{1}{3} P_{ss} - P_{11} - (C - 2\mathcal{A}\varepsilon_h) a_{11} \frac{2}{3} \varepsilon_h - \frac{\partial}{\partial x_2} \frac{\overline{u_1^2}}{q^2} \frac{u_s u_s u_2}{2} - \frac{1}{2} \nu \frac{\partial^2 \overline{u_1^2}}{\partial x_2^2} \quad (8)$$

0 if $(\Pi_a)_{\text{wall}} = 2/3$

* In (8)-(11) $P_{ij} = \overline{u_i u_k \partial U_j / \partial x_k} - \overline{u_i u_k \partial U_i / \partial x_k}$ represents the production of the turbulent stresses by mean motion, x_2 measures the distance from the wall, ε_h is the homogeneous part of the turbulent dissipation rate defined by eq.(17) and \mathcal{A} , C , and \mathcal{F} are scalar functions that depend on the anisotropy invariants and the turbulent Reynolds number

$$\begin{aligned} \frac{\partial \overline{u_2^2}}{\partial t} &= a_{22} P_{ss} - \frac{1}{3} \overline{FP}_{ss} - (C - 2\mathcal{A}\varepsilon_h) a_{22} - \frac{2}{3} \varepsilon_h \\ &\quad - \frac{\partial}{\partial x_2} \frac{\overline{u_2^2}}{q^2} \frac{\overline{u_s u_s u_2}}{2} - \frac{1}{2} \nu \underbrace{\frac{\partial^2 \overline{u_2^2}}{\partial x_2^2}}_{0 \text{ if } (\Pi_a)_{\text{wall}} = 2/3} \end{aligned} \quad (9)$$

$$\begin{aligned} \frac{\partial \overline{u_3^2}}{\partial t} &= a_{33} P_{ss} - \frac{1}{3} \overline{FP}_{ss} - (C - 2\mathcal{A}\varepsilon_h) a_{33} - \frac{2}{3} \varepsilon_h \\ &\quad - \frac{\partial}{\partial x_2} \frac{\overline{u_3^2}}{q^2} \frac{\overline{u_s u_s u_2}}{2} - \frac{1}{2} \nu \underbrace{\frac{\partial^2 \overline{u_3^2}}{\partial x_2^2}}_{0 \text{ if } (\Pi_a)_{\text{wall}} = 2/3} \end{aligned} \quad (10)$$

$$\begin{aligned} \frac{\partial \overline{u_1 u_2}}{\partial t} &= P_{12} - a_{12} P_{ss} - \overline{FP}_{12} - (C - 2\mathcal{A}\varepsilon_h) a_{12} \\ &\quad - \frac{\partial}{\partial x_2} \frac{\overline{u_1 u_2}}{q^2} \frac{\overline{u_s u_s u_2}}{2} - \frac{1}{2} \nu \underbrace{\frac{\partial^2 \overline{u_1 u_2}}{\partial x_2^2}}_{0 \text{ if } (\Pi_a)_{\text{wall}} = 2/3} \end{aligned} \quad (11)$$

suggest that the viscous diffusion process can almost be neglected, $\partial^2 \overline{u_i u_j} / \partial^2 x_2^2 = 0$, forcing turbulence to tend towards the axisymmetric state with the streamwise intensity larger than in the other two directions, $\overline{u_1^2} > \overline{u_2^2} > \overline{u_3^2}$. Since in axisymmetric turbulence there is no shear stress $\overline{u_1 u_2}$, it is to be expected that for large DR there will be no traditional mechanism of the energy production $P_k = \overline{u_1 u_2} \partial \overline{U_1} / \partial x_2$ which ensures self-maintenance of turbulence in wall-bounded flows.

The system (8)-(11) therefore permits an insight into the two important issues of turbulent DR that need to be distinguished: modifications of turbulence induced in the region of the viscous sublayer are of a causal nature and the significant reduction of turbulent energy production in the flow region away from the wall is a consequence of the mechanism associated with DR. Under these circumstances, turbulence can persist in polymer flows only if interaction between the polymers and turbulence induces additional polymers stresses. Thus, the evolution of turbulence in drag-reducing flows resembles the reverse transition process in the limit when $\text{Re} \rightarrow \text{Re}_{\text{crit}}$ as illustrated in fig. 17.

The specific process by which an increase in the anisotropy of turbulence influences DR is related to the ability of dilute flexible polymers to decrease the contribution of turbulence to the average energy dissipation rate. For a pipe flow this can be expressed as the rate of work done against the wall shear stress per unit mass of fluid:

$$\overline{\varepsilon} = \frac{\tau_w \pi D L \overline{U}_B}{\rho \pi \frac{1}{4} L D^2} - \frac{4 \overline{u_\tau^2} \overline{U}_B}{D} \quad (12)$$

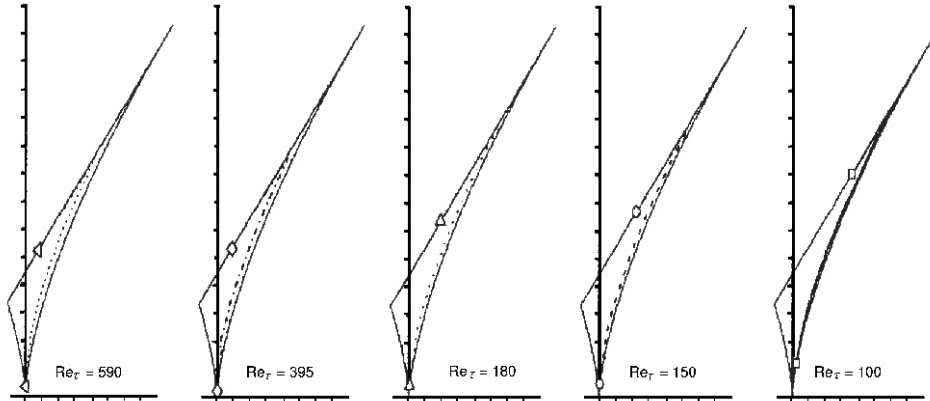


Figure 17. Anisotropy invariant mapping of turbulence in a channel flow. Data which correspond to low Reynolds number (based on the channel half-width and the wall friction velocity) show the trend as $Re \rightarrow Re_{crit}$ towards the theoretical solution valid for small, neutrally stable, statistically stationary axisymmetric disturbances [32]

where D and L are the pipe diameter and its length, respectively, \bar{U}_B represents bulk velocity, τ_w corresponds to the wall shear stress, $\tau_w = \mu(\partial \bar{U}_1 / \partial x_2)_0$, and u_τ is the wall friction velocity, $u_\tau = (\tau_w / \rho)^{1/2}$. From this equation, we may conclude that for a given mean flow (\bar{U}_B) and pipe diameter (D), only a decrease $\bar{\varepsilon}$ in ensures DR. It is therefore not surprising that measurements of the energy spectra of turbulence in drag-reducing flows display attenuation of fluctuations at high wave numbers (small-scales) across the entire flow [17]. These fluctuations contribute substantially not only to $\bar{\varepsilon}$ but also to the dynamics of the dissipation process, which are extremely complicated.

Determination of the relaxation time of a polymer for maximum drag reduction

In the previous section, we provided an explanation for the physical mechanism that causes turbulent DR by polymers. It is associated with modifications of turbulence at small scales by changes in the molecular structure of a polymer. It is therefore reasonable to assume that turbulent motions at high wave numbers are responsible for interaction between turbulence and a polymer. These motions are characterized by Kolmogorov's length scale, defined as:

$$\eta_K = \frac{\nu^3}{\varepsilon}^{1/4} \tag{13}$$

and additional scales which can be derived from ν and η_K :

velocity scale $u_K = v/\eta_K$,
 time scale $t_K = \eta_K^2 / \nu$, and
 pressure scale $p_K = \rho v^2/\eta_K$.

To ensure that the polymer produces DR, the characteristic time-scale of turbulence ($t_{\text{tur}} = t_K$) must be smaller than the relaxation time of a polymer (t_{pol}) in order to activate rolled-up chains of a polymer to unroll and in this way initialize DR [2]. This requirement may be formulated in the form:

$$t_K < t_{\text{pol}} \quad (14)$$

Using the well-known relationship for interpretation of the turbulent dissipation rate in terms of the energy ($2k = q^2 = u_s u_s$) and the Taylor microscale (λ) that holds in homogeneous turbulence:

$$\varepsilon = 5\nu \frac{q^2}{\lambda^2} \quad (15)$$

and from expression (13) we find:

$$t_K = \frac{\sqrt{5}}{5} \frac{\lambda}{q} \quad (16)$$

It is possible to show, using the two-point correlation technique [34], that the turbulent dissipation rate in wall-bounded flows may be interpreted in terms of the Taylor microscale as follows:

$$\varepsilon = \frac{1}{4} \nu \frac{\partial^2 q^2}{\partial x_k \partial x_k} = \underbrace{5\nu \frac{q^2}{\lambda^2}}_{\varepsilon_h} \quad (17)$$

Exploring the series expansion for the instantaneous velocity fluctuations about the wall [35]:

$$\begin{aligned} u_1 &= a_1 x_2 + a_2 x_2^2 + \dots \\ u_2 &= b_2 x_2^2 + \dots \quad \text{as } x_2 \rightarrow 0 \\ u_3 &= c_1 x_2 + c_2 x_2^2 + \dots \end{aligned} \quad (18)$$

where the coefficients a_i , b_i , and c_i are functions of time and space coordinates x_1 and x_3 , it is possible to show that λ and q are linear functions of the distance from the wall:

$$\begin{aligned} \lambda &= \sqrt{10} x_2 \\ q &= \sqrt{a_1^2 + c_1^2} x_2 \quad \text{as } x_2 \rightarrow 0 \end{aligned} \quad (19)$$

For pipe and channel flows, experimental investigations and numerical simulations indicate that the limiting behaviour of turbulence intensities close to the wall is nearly independent of the Reynolds number [36, 37]:

$$\begin{aligned} \sqrt{u_1^2} / \bar{U}_1 &= 0.4 \\ \sqrt{u_3^2} / \bar{U}_1 &= 0.2 \end{aligned} \quad \text{as } x_2 \rightarrow 0 \quad (20)$$

This behaviour yields:

$$\bar{a}_1^2 = 0.16 \frac{u_\tau^4}{\nu^2} \quad (21)$$

$$\bar{c}_1^2 = 0.04 \frac{u_\tau^4}{\nu^2} \quad (22)$$

From the above limiting behaviour of intensity components close to the wall, we deduce from expression (16) the time-scale t_K of turbulence at the wall:

$$(t_K)_{\text{wall}} = \sqrt{10} \frac{\nu}{u_\tau^2} \quad (23)$$

Another estimate of the time-scale t_K follows from consideration of turbulence at the pipe centreline. For this flow region, experiments show that all three intensity components are nearly equal and scale with the wall friction velocity [27, 36]:

$$\sqrt{u_1^2} = \sqrt{u_2^2} = \sqrt{u_3^2} = 0.75 u_\tau \quad (24)$$

This experimental evidence suggests the relation for the upper estimation of the time-scale t_K :

$$(t_K)_{\text{center}} = 0.265 (R_\lambda)_{\text{center}} \frac{\nu}{u_\tau^2} \quad (25)$$

where $(R_\lambda)_{\text{center}}$ is the turbulent Reynolds number $R_\lambda = q / \nu$ at the pipe centreline, which can be calculated approximately using the correlation (shown in fig. 18) suggested by Jovanović and Pashtropanska [38]:

$$R_\lambda = 1.996 \frac{u_\tau D}{\nu} - 0.108 \quad (26)$$

By requiring that the relaxation time of the polymer t_{pol} is larger than expression (23) and smaller than or equal to expression (25):

$$\sqrt{10} \frac{\nu}{u_\tau^2} < t_{\text{pol}} \leq 0.265 (R_\lambda)_{\text{center}} \frac{\nu}{u_\tau^2} \quad (27)$$

we obtain the condition that needs to be fulfilled in order that polymer molecules become substantially elongated, resulting in maximum DR. The lower bound for t_K expression (23) is far more representative than the upper bound expression (25), since effects close

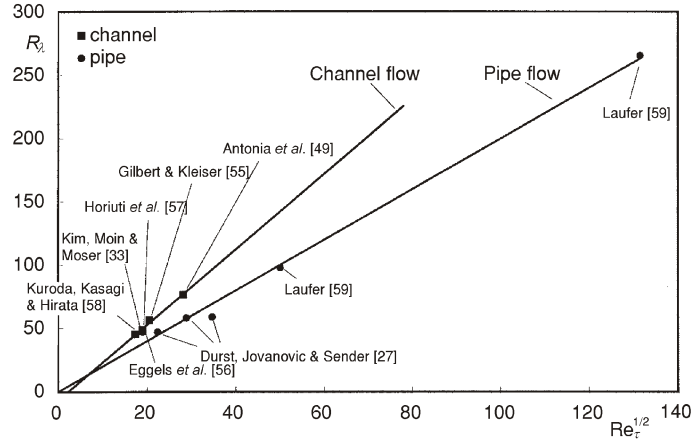


Figure 18. Cross plot of R_λ versus $Re_\tau^{1/2}$ for fully developed turbulent pipe ($Re_\tau = u_\tau D/\nu$) and channel flows, from Jovanović and Pashtrapanska [38]

to the wall are of the causal nature for nearly all production of turbulence in wall-bounded flows and therefore strongly influence its contribution to the viscous drag.

Figure 19 shows experimental results of Durst *et al.* [39] for polymer drag reduction, defined in terms of the dimensionless coefficients of resistance λ :

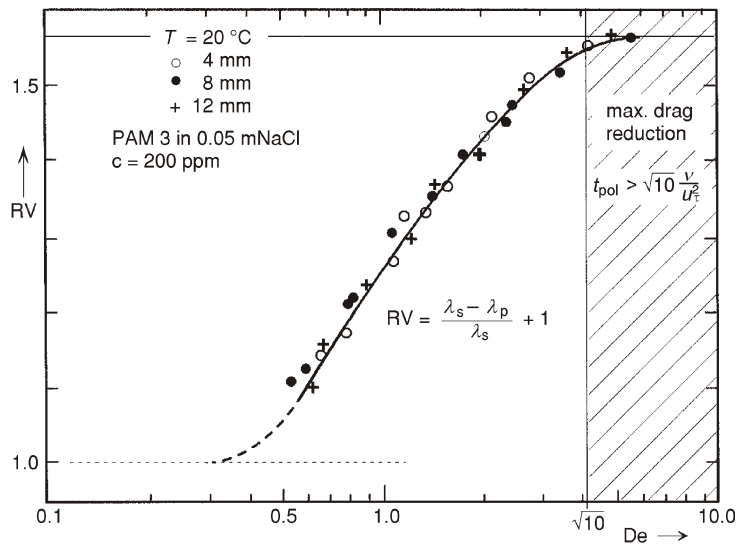


Figure 19. Drag reduction in pipes of different diameters versus a polymer time scale normalized by a viscous time scale ν / u_τ^2 in a fully developed turbulent pipe flow (from Durst *et al.* [39]) and the predicted value of a Deborah number (De) for the maximum DR effect

$$\frac{\Delta p}{L} = \frac{\lambda}{D} \frac{1}{2} \rho \overline{U_B}^2 \quad (28)$$

for the solvent (λ_s) and a dilute polymer solution (λ_p) versus the Deborah number (De):

$$\text{De} = \frac{t_{\text{pol}}}{\frac{v}{u_\tau^2}} \quad (29)$$

These experimental results, which were obtained in a turbulent pipe flow at moderate Reynolds numbers, confirm that maximum DR is already reached when the De exceeds a value of about $\text{De} = \sqrt{10}$. This finding is in close agreement with the conclusion that emerges from the time-scale argumentation discussed above and is in agreement with the lower bound of the constraint derived expression (27) for the relaxation time of a polymer. Considering that the molecular weight of a polymer (M) is distributed according to the probability density distribution the onset of DR at $\text{De} = 0.5$ is not surprising. If the right-hand side tail of the probability density distribution of the molecular weight of a polymer extends to three times of \overline{M} then the requirement $t_{\text{pol}} = (t_K)_{\text{wall}}$, which corresponds to \overline{M} , together with the Zimm relation for t_{pol} suggests that the onset of DR starts already at $\text{De} = 0.44$ (see also fig. 14)

The optimum concentration of a polymer

If we assume that the entire interaction between a polymer and turbulence is localized in the dissipation range of the spectrum, this implies that the volume occupied by fluid motions which scale with Kolmogorov's variables (η_K , t_K , u_K , and p_K) should be equal to the volume of a polymer in order to obtain maximum DR. Since the small-scale structure of turbulence is (believed to be) universal for all turbulent flows, the volume occupied by it can be determined by considering well-established results which hold for isotropic turbulence.

For isotropic turbulence at large Reynolds numbers, the turbulent dissipation ε may be related to the integral length scale of the energy containing range [40, 41]:

$$\varepsilon = 0.192 \frac{q^3}{L_f}, \quad R_\lambda \gg 1 \quad (30)$$

At very low Reynolds numbers, *e. g.* in the final decay period of classical grid-generated turbulence, the expression for ε can be derived analytically [42]:

$$\varepsilon = 1.959 v \frac{q^2}{L_f^2}, \quad R_\lambda \ll 1 \quad (31)$$

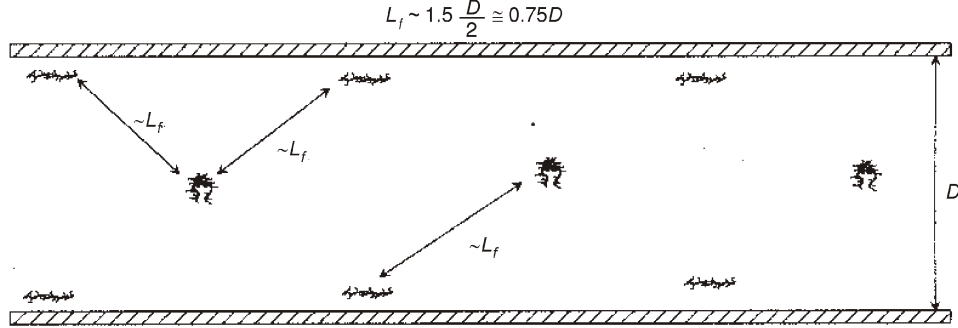


Figure 20. The arrangement of polymer molecules for maximum DR in a fully developed pipe flow is dictated by spatial intermittency of turbulence at small scales

Following the suggestion of Rotta [43], we combine expressions (30) and (31) to obtain an interpolation equation for ε valid for low and large Reynolds numbers:

$$\varepsilon = 1959\nu \frac{q^2}{L_f^2} + 0.192 \frac{q^3}{L_f} \quad (32)$$

Expressing ε in terms of Taylor's microscale, using expression (15), with (32) we are in position to correlate the length scale ratio λ/L_f in terms of the turbulent Reynolds number:

$$\frac{\lambda}{L_f} = 0.049R_\lambda + \frac{1}{2} (0.009604R_\lambda^2 + 10208)^{1/2} \quad (33)$$

which attains a maximum value of 1.597 when $R_\lambda = 0$ and vanishes for $R_\lambda = \infty$. Using expressions (13) and (15), the above ratio λ/L_f can be transformed to the ratio of Kolmogorov's length scale to the length scale L_f :

$$\frac{\eta_K}{L_f} = 0.0327R_\lambda^{1/2} + 0.3343R_\lambda^{-1/2} (0.009604R_\lambda^2 + 10208)^{1/2} \quad (34)$$

Experimental investigations of statistical properties of the fine scale structure of turbulence by Batchelor and Townsend [44] and Kuo and Corrsin [45] reveal that the mean separation between flow regions in space where turbulent motions correlate well with Kolmogorov's length scale is comparable to the (integral) length scale L_f of turbulence (see fig. 20). This finding implies that there is one Kolmogorov structure (η_K) inside the large-scale structure (L_f), so that the volume occupied by a polymer (c) relative to the volume of entire fluid (V) can be estimated as follows:

$$\frac{c}{V} = \left(\frac{\eta_K}{L_f} \right)^3 [0.0327R_\lambda^{1/2} + 0.3343R_\lambda^{-1/2} (0.009604R_\lambda^2 + 10208)^{1/2}]^3 \quad (35)$$

It is important to note that the above expression predicts a decrease of c/V with increasing Reynolds number.

Using expressions (26), (35) and the Blasius correlation formula for the friction coefficient, the optimum concentration of a polymer for the maximum DR effect was predicted for pipe flow and in fig. 21 the results are compared with measurements carried out by Tilli *et al.* [46] for Polyacrylic acid (PAA) dissolved in water. The predicted concentration is seen to follow very closely the measurements performed in the Reynolds number range $Re = 1.0 \cdot 10^4 - 7.2 \cdot 10^4$.

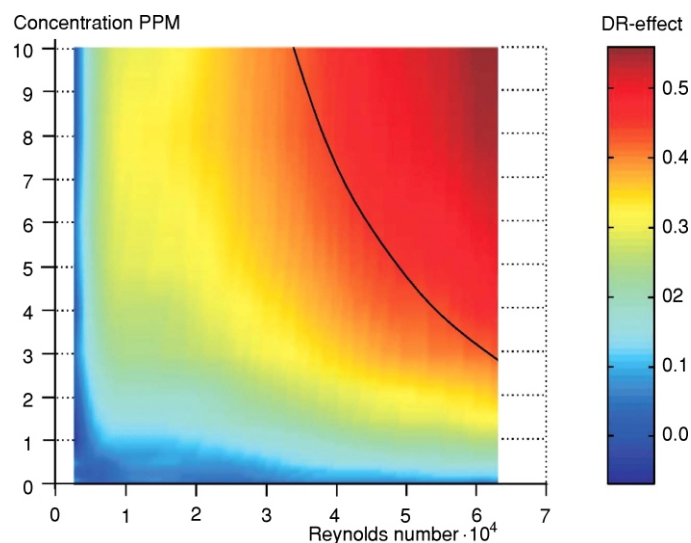


Figure 21. Measured DR effects at different PAA concentrations in aqueous solutions as a function of the Reynolds number; from Tilli *et al.* [46]. The solid line represents prediction of the optimum concentration of a polymer for the maximum DR effect

Conclusions

High spatial resolution laser-Doppler measurements were performed in a refractive index-matched pipe flow facility in order to provide experimental evidence for the chief mechanism responsible for polymer DR. Special care was taken to maintain well-controlled flow conditions during the experiments and to account for all possible interferences that can influence the interpretation of the measured LDA signals. The experimental results for the mean velocity and turbulence intensity components obtained deep in the viscous sublayer permitted the evolution of turbulence to be traced across the ani-

sotropy invariant map. Anisotropy invariant mapping of turbulence in the viscous sublayer reveals that with decrease of DR the anisotropy near the wall decreases along the line which characterizes the two-component state starting from nearly the one-component limit which correspond to large DR and finishing approximately midway between the one-component limit and the isotropic two-component limit for vanishing DR effect. These observations, extracted from the experimental results, are in close agreement with the theoretical analysis and support the notion that turbulent DR by dilute addition of high polymers is associated with the ability of long-chain polymers to induce an increase in the anisotropy of turbulence in close proximity to the wall.

Statistical analysis of the dynamic equations for turbulent stresses, using the two-point correlation technique and invariant theory, have been performed to investigate polymer DR phenomena. By considering local stretching of the molecular structure of a polymer by small-scale turbulent motions in the region of the viscous sublayer, a conceptual scenario was inferred from theory for the behavior of a polymer and its interaction with turbulence that leads to significant DR effects. According to this scenario, the stretching process is responsible for the re-structuring of turbulence at small scales close to the wall by forcing it to satisfy local axisymmetry with invariance under rotation about the axis aligned with the mean flow. Analytical considerations lead to the conclusion that under these circumstances turbulence at the wall tends towards the one-component limit and when it reaches this limiting state turbulence must be entirely suppressed near the wall. In addition to these findings, qualitative analysis of the turbulent transport equations, when projected into the invariant space, suggested that DR by high polymers mimics reverse transition from the fully turbulent state towards the laminar flow state. These analytical deductions were supported by all available results from direct numerical simulations of wall-bounded turbulent flows including those of non-Newtonian fluids.

Examination of the statistical dynamics of the turbulent stresses for conditions of large DR suggest that suppression of the viscous diffusion process at the wall is the major cause for polymer DR and significant reduction of turbulent energy production in the flow region away from the wall can be regarded as a logical consequence. These effects are reflected in a significant reduction of the average turbulent dissipation rate $\bar{\varepsilon}$ which controls the turbulent drag. These findings are illustrated in fig. 22, which shows distributions of the root mean square of the streamwise vorticity fluctuations $(\omega_1^2)^{1/2}$, which are the largest contribution to the turbulent dissipation rate, $\varepsilon = \omega_i \omega_i$, in a turbulent channel flow.

Parameterisation of the mechanism associated with polymer DR was accomplished by considering the elastic behaviour of a polymer and accounting for spatial intermittency of turbulence at small scales. The analysis assumed that the interaction between a polymer and turbulence is localized in motions at small scales which are of the intermittent nature and responsible for the viscous destruction of the turbulent dissipation rate. Favourable agreement was obtained between predictions, based on theoretical considerations, and available experimental results for the relaxation time-scale of a polymer and its concentration that produce the maximum DR effect.

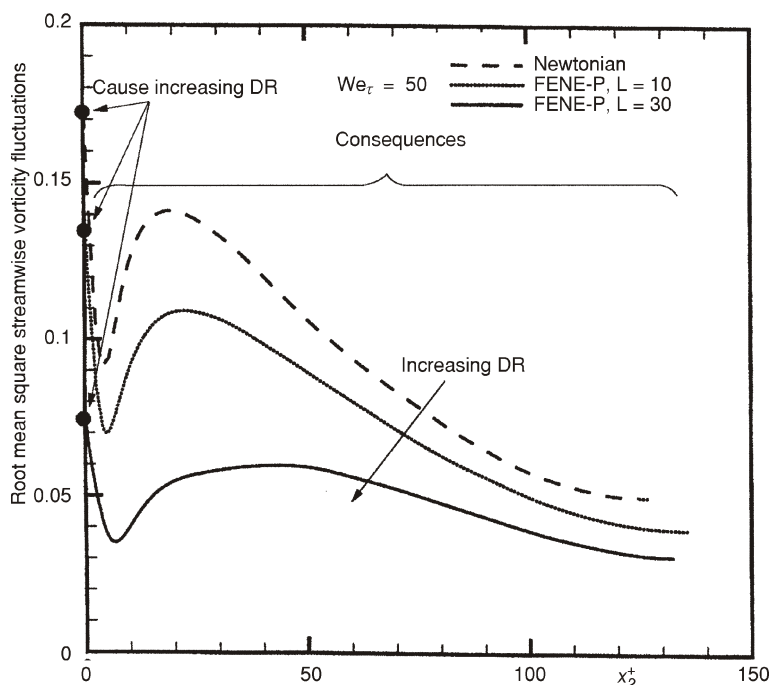


Figure 22. Illustration of the chief mechanism responsible for polymer DR utilizing the results of direct numerical simulations of Dimitropulos *et al.* [20]

Acknowledgments

The authors gratefully acknowledge the donation of the required oil by ESSO AG, Refinery Ingolstadt, Germany.

References

- [1] Metzner, A. B., Park, M. G., Turbulent Flow Characteristics of Viscoelastic Fluids. *J. Fluid Mech.*, 20 (1964), pp. 291-303
- [2] Lumley, J. L., Drag Reduction by Additives, *Annu. Rev. Fluid Mech.*, 1 (1969), pp. 367-384
- [3] Lumley, J. L., Drag Reduction in Turbulent Flow by Polymer Additives, *J. Polymer Sci. Macrom. Rev.*, 7 (1973), pp. 363-390
- [4] Virk, P. S., Drag Reduction Fundamentals, *AIChE J.*, 21 (1975), pp. 625-656
- [5] Berman, N. S., Drag Reduction by Polymers, *Annu. Rev. Fluid Mech.*, 10 (1978), pp. 47-64
- [6] Tabor, M., Gennes, P. G. de., A Cascade Theory of Drag Reduction, *Europhys. Lett.*, 2 (1986), pp. 519-522
- [7] Ryskin, G., Turbulent Drag Reduction by Polymers: a Quantitative Theory, *Phys. Rev. Lett.*, 59 (1987), pp. 2059-2062

- [8] Thirumalai, D., Bhattacharjee, J. K., Polymer-Induced Drag Reduction in Turbulent Flows, *Phys. Rev. E*, 53 (1996), pp. 546-551
- [9] Sreenivasan, K. R., White, C. M., The Onset of Drag Reduction by Dilute Polymer Additives and the Maximum Drag Reduction Asymptote, *J. Fluid Mech.*, 409 (2000), 149-164
- [10] Rudd, M. J., Velocity Measurements with a Laser-Doppler Meter on the Turbulent flow of a Dilute Polymer Solution, *J. Fluid Mech.*, 51 (1972), pp. 673-685
- [11] Logan, S. E., Laser Velocimeter Measurements of Reynolds Stress in Dilute Polymer Solutions, *AIAA J.*, 10 (1972), pp. 962-964
- [12] Reischman, M. A., Tiederman, W. G., Laser-Doppler Anemometer Measurements in Drag Reduction Channel Flow, *J. Fluid Mech.*, 70 (1975), pp. 369-392
- [13] Luchik, T. S., Tiederman, W. G., Turbulent Structure in Low-Concentration Drag-Reducing Channel Flow, *J. Fluid Mech.*, 198 (1988), pp. 241-263
- [14] Walker, D. T., Tiederman, W. G., Turbulent Structure in a Channel Flow with Polymer Injection at the Wall, *J. Fluid Mech.*, 204 (1990), pp. 377-403
- [15] Willmarth, W. W., Wei, T., Lee, O., Laser Anemometer Measurements of Reynolds Stress in a Turbulent Channel Flow with Drag Reducing Polymer Additives, *Phys. Fluids*, 30 (1987), pp. 933-935
- [16] Wei, T., Willmarth, W. W., Modifying Turbulent Structure with Drag-Reducing Polymer Additives in Turbulent Channel Flows, *J. Fluid Mech.*, 245 (1992), pp. 619-641
- [17] Warholic, M. D., Massah, H., Hanratty, T. J., Influence of Drag-Reducing Polymers on Turbulence: Effects of Reynolds Number, Concentration and Mixing, *Exp. Fluids*, 27 (1999), pp. 461-472
- [18] Toonder, J. M. J. den, Hulsen, M. A., Kuiken, G. D. C., Nieuwstadt, F., Drag Reduction by Polymer Additives in Turbulent Pipe Flow: Numerical and Laboratory Experiments, *J. Fluid Mech.*, 337 (1997), pp. 193-231
- [19] Sureshkumar, R., Beris, A. N., Handler, R. A., Direct Numerical Simulations of Turbulent Channel Flow of a Polymer Solution, *Phys. Fluids*, 9 (1997), pp. 743-755
- [20] Dimitropoulos, C. R., Suresikumar, R., Beris, A. N., Direct Numerical Simulation of Viscoelastic Turbulent Channel Exhibiting Drag Reduction: Effect of the Variation of Rheological Parameters, *J. Non-Newtonian Fluid Mech.*, 79 (1998), pp. 443-468
- [21] Sibilla, S., Baron, A., Polymer Stress Statistics in the Near-Wall Turbulent Flow of a Drag-Reducing Solution, *Phys. Fluid*, 14 (2002), pp. 1123-1136
- [22] Angelis, E. D., Casciola, C. M., Piva, R., DNS of Wall Turbulence: Dilute Polymers and Self-Sustaining Mechanisms, *Computers & Fluids*, 31 (2002), pp. 495-507
- [23] Dubief, Y., Numerical Simulation of Turbulent Polymer Solutions, *Ann. Res. Briefs*, Center for Turbulence Research, Stanford University, 2002, pp. 377-388
- [24] Dubief, Y., White, C., Terrapon, V., Shaqfeh, E., Moin, P., Lele, S., On the Coherent Drag-Reducing and Turbulence Enhancing Behaviour of Polymers in Wall Flows, *J. Fluid Mech.*, 514 (2004), pp. 271- 280
- [25] Jovanović, J. The Statistical Dynamics of Turbulence, Springer-Verlag, Berlin-Heidelberg, 2004
- [26] Jovanović, J., Hillerbrand, R., On Peculiar Property of the Velocity Fluctuations in Wall-Bounded Flows, *Thermal Science*, 9 (2005), 1, pp. 3-12 (in this issue)
- [27] Durst, F., Jovanović, J., Sender, J., LDA Measurements in the Near-Wall Region of a Turbulent Pipe Flow, *J. Fluid Mech.*, 295 (1995), pp. 305-335
- [28] Mansour, N. N., Moser, R. D., Kim, J., Fully Developed Turbulent Channel Flow Simulations, in: AGARD Advisory Report 345, 1998, pp. 119-121
- [29] Koskinen, K. K., On Investigating Turbulent Reactive Flows: Case Studies of Combustion and Drag Reduction by Polymer Additives, Ongoing Ph. D. thesis, Tampere University of Technology, Tampere, Finland, 2004
- [30] Lumley, J. L., Newman, G., The Return to Isotropy of Homogeneous Turbulence, *J. Fluid Mech.*, 82 (1977), pp. 161-178

- [31] Lumley, J. L., Computational Modeling of Turbulent Flows, *Adv. Appl. Mech.*, 18 (1978), pp. 123-176
- [32] Jovanović, J., Hillerbrand, R., Pashtrapanska, M., The Statistical Analysis of the Origin of Turbulence Using Numerical Databases, *KONWIHR Quartl* 31 (2001), pp. 6-8
- [33] Kim, J., Moin, P., Moser, R., Turbulence Statistics in a Fully Developed Channel Flow at Low Reynolds Numbers, *J. Fluid Mech.*, 177 (1987), pp. 133-166
- [34] Jovanović, J., Ye, Q.-Y., Durst, F., Statistical Interpretation of the Turbulent Dissipation Rate in Wall-Bounded Flows, *J. Fluid Mech.*, 293 (1995), pp. 321-347
- [35] Monin, A. S., Yaglom, A. M., The Statistical Fluid Mechanics, Vol. 1, MIT Press, Cambridge, MA, USA, 1987
- [36] Durst, F., Fischer, M., Jovanović, J., Kikura, H., Methods to Set Up and Investigate Low Reynolds Number, Fully Developed Turbulent Plane Channel Flows, *J. Fluids Eng.*, 120 (1998), pp. 496-503
- [37] Fischer, M., Jovanović, J., Durst, F., Reynolds Number Effects in the Near-Wall Region of Turbulent Channel Flows, *Phys. Fluids*, 13 (2001), pp. 1755-1767
- [38] Jovanović, J., Pashtrapanska, M., On the Criterion for the Determination Transition Onset and Breakdown to Turbulence in Wall-Bounded Flows, *J. Fluids Eng.*, 2003, submitted
- [39] Durst, F., Hass, R., Interhal, W., Keck, T., The Influence of Polymers of Fluid Flows: Mechanisms and Practical Applications (in German), *Chem.-Ing.-Tech.*, 54 (1982), pp. 213-221
- [40] Kolmogorov, A. N., Local Structure of Turbulence in an Incompressible Fluid at Very High Reynolds Numbers (in Russian), *Dokl. Akad. Nauk SSSR*, 30 (1941), pp. 299-303
- [41] Sreenivasan, K. R., On the Scaling of the Turbulence Energy Dissipation Rate, *Phys. Fluids*, 27 (1984), pp. 1048-1051
- [42] Hinze, J. O., Turbulence, 2nd ed., McGraw Hill, New York, 1975
- [43] Rotta, J., Statistical Theory of Nonhomogeneous Turbulence (in German), *Z. Physik*, 129 (1951), pp. 547-572
- [44] Batchelor, G. K., Townsend, A. A., Decay of Vorticity in Isotropic Turbulence, *Proc. Roy. Soc. A*, 190 (1947), p. 534
- [45] Kuo, A. Y., Corrsin, S., Experiments on Internal Intermittency and Fine-Structure Distribution Functions in Fully Turbulent Fluid, *J. Fluid Mech.*, 50 (1971), pp. 285-319
- [46] Tilli, M., Maaranen, J., Timonen, J., Kataja, M., Korppi-Tommola, J., Effect Mechanisms of DR Molecules, Technical Report, University of Jyväskylä, Finland, 2003
- [47] George, W. K., Hussein, H. J., Locally Axisymmetric Turbulence, *J. Fluid Mech.*, 233 (1991), pp. 1-23
- [48] Schenck, T., Jovanović, J., Measurements of the Instantaneous Velocity Gradients in Plane and Axisymmetric Wake Flows, *J. Fluids Eng.*, 124 (2002), pp. 143-153
- [49] Antonia, R. A., Teitel, M., Kim, J., Browne, L. W. B., Low-Reynolds-Number Effects in a Fully Developed Turbulent Channel Flow, *J. Fluid Mech.*, 236 (1992), pp. 579-605
- [50] Chou, P. Y., On the Velocity Correlation and the Solution of the Equation of Turbulent Fluctuation, *Quart. Appl. Math.*, 3 (1945), pp. 38-54
- [51] Kolovandin, B. A., Vatutin, I. A., On Statistical Theory of Non-Uniform Turbulence, Presented at International Seminar on Heat and Mass Transfer in Flows with Separated Regions and Measurement Techniques, Herceg-Novi, Yugoslavia, September 1-13, 1969
- [52] Spalart, P. R., Numerical Study of Sink-Flow Boundary Layers, *J. Fluid Mech.*, 172 (1986), pp. 307-328
- [53] Spalart, P. R., Direct Simulation of a Turbulent Boundary Layer up to $Re_\theta = 1410$, *J. Fluid Mech.*, 187 (1988), pp. 61-98
- [54] Moser, R. D., Kim, J., Mansour, N. N., Direct Numerical Simulation of Turbulent Channel Flow up to $Re_\tau = 590$, *Phys. Fluids*, 11 (1999), pp. 943-945
- [55] Gilbert, N., Kleiser, L., Turbulence Model Testing with the Aid of Direct Numerical Simulation Results, *Proceedings*, Eighth Symposium on Turbulent Shear Flows, Munich, Germany, 1991, pp. 26.1.1-26.1.6

- [56] Eggels, J. G. M., Unger, F., Weiss, M. H., Westerweel, J., Adrian, R. J., Friedrich, R., Nieuwstadt, F. T. M., Fully Developed Turbulent Pipe Flow: a Comparison between Direct Numerical Simulation and Experiment, *J. Fluid Mech.*, 268 (1994), pp. 175-209
- [57] Horiuti, K., Establishment of the Direct Numerical Simulation Data Base of Turbulent Transport Phenomena, Ministry of Education, Science and Culture Japan, Co-Operative Research No. 012302043, 1992, <http://www.thtlab.t.u-tokyo.ac.jp/>
- [58] Kuroda, A., Kasagi, N., Hirata, M., Direct Numerical Simulation of the Turbulent Plane Couette-Poiseuille Flows: Effect of Mean Shear on the Near Wall Turbulence Structures, *Proceedings*, Ninth Symposium on Turbulent Shear Flows, 1993, Kyoto, 8.4.1-8.4.6, <http://www.thtlab.t.u-tokyo.ac.jp/>
- [59] Laufer, J., The Structure of Turbulence in Fully Developed Pipe Flow, NACA Tech. Note 2954, 1953
- [60] Koskinen, K. K., On Investigating Turbulent Reactive Flows: Case Studies of Combustion and Drag Reduction by Polymer Additives, Ongoing Ph. D. thesis, Tampere University of Technology, Tampere, Finland, 2004

Authors' address:

*J. Jovanović, B. Frohnappel,
M. Pashtrapanska, F. Durst*

Lehrstuhl für Strömungsmechanik,
Universität Erlangen-Nürnberg
Cauerstrasse 4, D-91058 Erlangen,
Germany

Corresponding author (J. Jovanović):
E-mail: jovan.jovanovic@nzmil.uni-erlangen.de